JOURNAL OF GEOPHYSICAL RESEARCH, VOL. 113, C07004, doi:10.1029/2007JC004564, 2008

Antarctic sea ice variability and trends, 1979–2006

D. J. Cavalieri[1] and C. L. Parkinson[1]

Received 20 September 2007; revised 6 March 2008; accepted 18 March 2008; published 1 July 2008.

[1] Analyses of 28 years (1979–2006) of Antarctic sea ice extents and areas derived from satellite passive microwave radiometers are presented and placed in the context of results obtained previously for the 20-year period 1979–1998. We present monthly averaged sea ice extents and areas, monthly deviations, yearly and seasonal averages, and their trends for the Southern Hemisphere as a whole and for each of five sectors: the Weddell Sea, the Indian Ocean, the western Pacific Ocean, the Ross Sea, and the Bellingshausen/Amundsen seas. The total Antarctic sea ice extent trend increased slightly, from 0.96 ± 0.61% decade^{-1} to 1.0 ± 0.4% decade^{-1}, from the 20- to 28-year period, reflecting contrasting changes in the sector trends. The eight additional years resulted in smaller positive yearly trends in sea ice extent for the Weddell Sea (0.80 ± 1.4% decade^{-1}), the western Pacific Ocean (1.4 ± 1.9% decade^{-1}), and the Ross Sea (4.4 ± 1.7% decade^{-1}) sectors, a lessening of the negative trend for the Bellingshausen/Amundsen seas (−5.4 ± 1.9% decade^{-1}) sector, and a shift from a negative trend to a positive trend for the Indian Ocean (1.9 ± 1.4% decade^{-1}) sector. The trends for the Southern Hemisphere as a whole and for the Ross Sea sector are significant at the 95% level, whereas the trend for the Bellingshausen/Amundsen seas sector is significant at the 99% level. A similar pattern of yearly trend changes for the two periods is also apparent in the sea ice area time series.

Citation: Cavalieri, D. J., and C. L. Parkinson (2008), Antarctic sea ice variability and trends, 1979–2006, *J. Geophys. Res.*, *113*, C07004, doi:10.1029/2007JC004564.

1. Introduction

[2] Satellite passive microwave observations of the Earth's polar sea ice cover have provided a wealth of information on its regional, seasonal, and interannual variabilities. A great deal of attention has been paid recently to the decline of the Arctic sea ice cover as observed by satellites over the past several decades [e.g., *Parkinson et al.*, 1999; *Stroeve et al.*, 2005; *Vinnikov et al.*, 2006]. In contrast to the Arctic, the total Antarctic sea ice cover has been gradually increasing from the mid-1970s through 2002 [*Cavalieri et al.*, 2003]. The amplitude and period of its interannual fluctuations have also been shown to be markedly different than those of the Arctic, suggesting that different processes are driving these changes [*Cavalieri et al.*, 1997]. Analyses of Arctic sea ice variability for the period 1979–2006 are presented in a companion paper [*Parkinson and Cavalieri*, 2008], whereas in this paper we present analyses for Antarctic sea ice variability for the same 28-year period.

[3] In this study we extend the 20-year (1979–1998) time series presented by *Zwally et al.* [2002] and discuss the differences in the Antarctic sea ice variabilities and trends observed between the 20-year and 28-year periods. Maps showing the average February and September sea ice concentrations over the 28-year period are shown in Figure 1. Much background material about Antarctic sea ice and the characteristics of each of the five sectors used in the analyses is given by *Zwally et al.* [2002] and is not repeated here. The emphasis in this study is on the changes that occurred from the previous 20-year time series results to the current 28-year results. In section 2 we present a brief description of the data sets used and the methods employed to derive the sea ice time series. In section 3 we present the results of our analyses for sea ice extents and sea ice areas. In section 4, a discussion of results and conclusions are presented.

2. Data Sources and Methods

[4] The time series presented in this study extend the satellite passive microwave data used by *Zwally et al.* [2002]. The base data set from which the ice extents and areas are calculated consists of sea ice concentration maps derived from the radiances obtained from the following satellite microwave radiometers: the Nimbus 7 Scanning Multichannel Microwave Radiometer (SMMR), which operated from 26 October 1978 through 20 August 1987, and the Defense Meteorological Satellite Program (DMSP) series of F8, F11, and F13 Special Sensor Microwave Imagers (SSMI). The F8 SSMI operated from 9 July 1987 through 18 December 1991; the F11 SSMI from 3 December 1991 through 30 September 1995; and

[1]NASA Goddard Space Flight Center, Greenbelt, Maryland, USA.

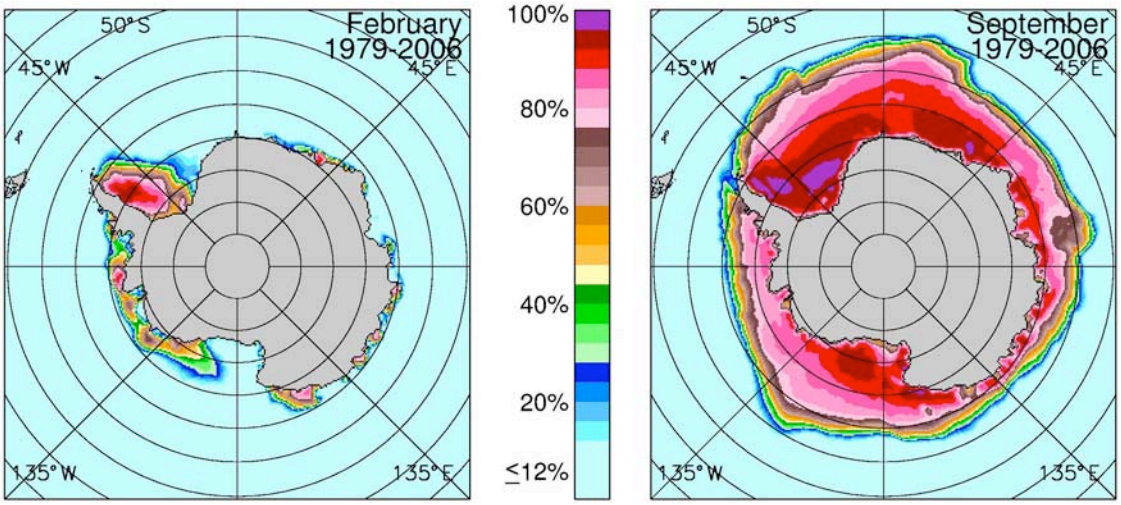

Figure 1. Southern Hemisphere 28-year average ice concentration maps for February and September, the months of average minimum and maximum sea ice extents, respectively.

the F13 SSMI from 3 May 1995 through 31 December 2006 and beyond.

[5] The problem of generating a long-term, consistent time series of sea ice extents and areas when working with sensors having different frequencies, different footprint sizes, different ascending node times, and different calibrations is considerable. The overall approach followed a method of matching sea ice parameters instead of attempting to match sensor radiances. Details of the approach, including filling data gaps, reducing land-to-ocean spillover effects, reducing weather effects over open ocean, and finally matching sea ice extents and areas for each pair of overlapping sensors, are discussed by *Cavalieri et al.* [1999]. Starting with the Nimbus 7 SMMR we matched each subsequent sensor with the previous sensor using the period of overlap to minimize the differences. While we did not have the desired complete year of overlap for each pair of sensors, we were able to reduce ice extent differences during periods of sensor overlap to 0.1% or less and ice area differences to 0.6% or less.

3. Results

[6] We present monthly averaged sea ice extents and areas for the Southern Hemisphere as a whole and also for each of five Southern Hemisphere sectors: the Weddell Sea, the Indian Ocean, the western Pacific Ocean, the Ross Sea, and the Bellingshausen/Amundsen seas (Figure 2). We also present for each sector and for the hemisphere monthly deviations of sea ice extents and areas, and yearly and seasonally averaged sea ice extents and areas and their trends.

[7] For the trends presented in this paper we calculate the ratio (R) of the estimated trend to its standard deviation for the purpose of providing a relative measure of the "significance" of all the trends. This provides a continuous measure of "significance" and is less arbitrary than the 95% or 99% levels of statistical significance generally used. Nonetheless, we do indicate these levels of significance in the trend tables to provide a reference for comparison with other published values. The levels of statistical significance are obtained using the Student's t-test with the null hypothesis of a zero trend and assuming 26 (28-2) degrees of freedom. The threshold values of R corresponding to the 95% and 99% levels of statistical significance are 2.06 and 2.78, respectively. It should be noted that the use of this statistical significance test has been criticized both for the use of the null hypothesis and the arbitrary levels of significance [e.g., *Nicholls*, 2001] and for issues related to the autocorrelation of the data [e.g., *Santer et al.*, 2000]. The use of these arbitrary levels of statistical significance in this study is only to provide a relative measure of the robustness of the trend to those trends with lower values of R.

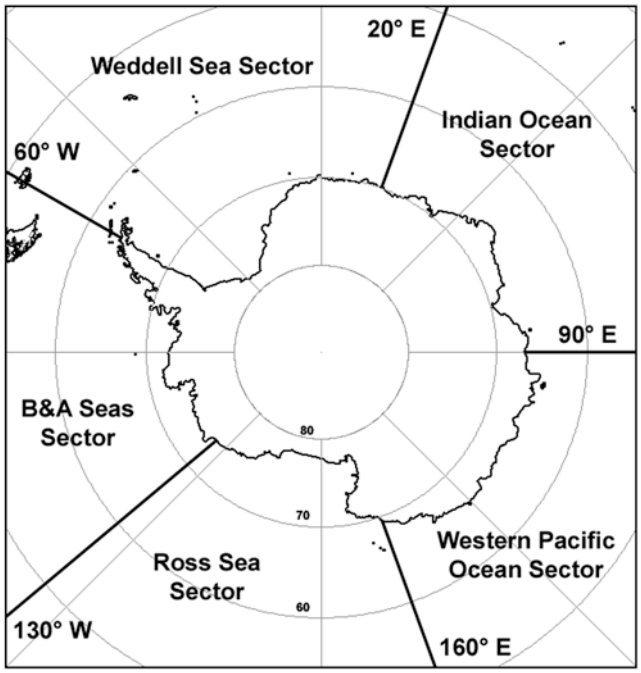

Figure 2. Southern Hemisphere sector map.

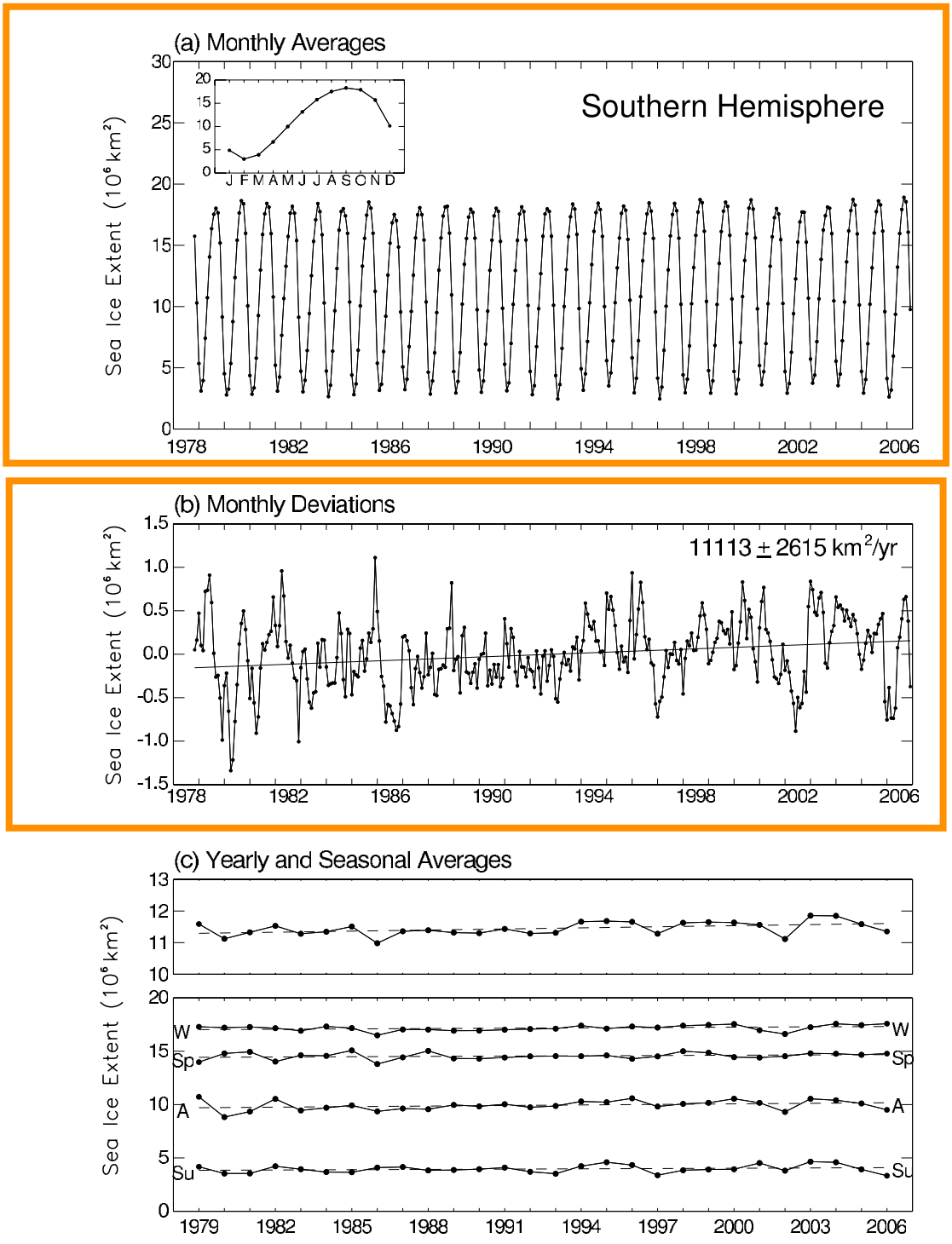

Figure 3. Time series of (a) monthly averages of sea ice extent for the Southern Hemisphere from November 1978 through December 2006. The inset shows the annual cycle computed from the 28 years of data, (b) monthly deviations of sea ice extent fitted with a linear least squares best fit trend line, (c) yearly and seasonal averages of sea ice extents with linear least squares best fit trend line. Summer averages (Su) are for January–March, autumn averages (A) are for April–June, winter averages (W) are for July–September, and spring averages (Sp) are for October–December.

3.1. Sea Ice Extents

3.1.1. Southern Hemisphere

[8] On average, over the 28-year period, maximum sea ice extent occurs in September, and minimum ice extent occurs in February (Figure 3a, inset). The monthly averages (Figure 3a) show a modest amount of variability from year to year, contrasting with much greater year-to-year variability within the individual sectors, shown later.

Table 1. Yearly and Seasonal Antarctic Sea Ice Extent Trends for the Period 1979–2006 With Estimated Standard Deviations[a]

Sector	Yearly		Winter (JAS)		Spring (OND)		Summer (JFM)		Autumn (AMJ)	
	10^3 km^2 a^{-1} (R)	Percent Decade^{-1}	10^3 km^2 a^{-1} (R)	Percent Decade^{-1}	10^3 km^2 a^{-1} (R)	Percent Decade^{-1}	10^3 km^2 a^{-1} (R)	Percent Decade^{-1}	10^3 km^2 a^{-1} (R)	Percent Decade^{-1}
SH	11.5 ± 4.6 (**2.50**)	1.0 ± 0.4	10.8 ± 5.9 (1.83)	0.6 ± 0.3	9.3 ± 7.2 (1.29)	0.6 ± 0.5	9.1 ± 8.5 (1.07)	2.4 ± 2.2	17.3 ± 10.5 (1.65)	1.8 ± 1.1
Weddell	3.3 ± 5.6 (0.59)	0.8 ± 1.4	−0.5 ± 8.0 (0.06)	−0.1 ± 1.3	−0.7 ± 7.9 (0.09)	−0.1 ± 1.5	8.6 ± 7.0 (1.23)	6.3 ± 5.1	6.1 ± 7.7 (0.79)	1.8 ± 2.2
Indian	3.5 ± 2.6 (1.35)	1.9 ± 1.4	5.6 ± 4.5 (1.24)	1.8 ± 1.5	5.8 ± 4.5 (1.28)	2.2 ± 1.7	0.7 ± 1.7 (0.41)	2.4 ± 5.8	1.8 ± 3.5 (0.51)	1.4 ± 2.8
W. Pacific	1.6 ± 2.2 (0.73)	1.4 ± 1.9	1.0 ± 3.9 (0.26)	0.6 ± 2.2	−1.8 ± 3.3 (0.55)	−1.3 ± 2.4	2.6 ± 2.5 (1.04)	6.2 ± 5.8	4.7 ± 2.6 (1.81)	4.6 ± 2.5
Ross	11.4 ± 4.6 (**2.48**)	4.4 ± 1.7	8.8 ± 5.6 (1.57)	2.3 ± 1.5	15.6 ± 6.2 (**2.52**)	4.9 ± 1.9	9.5 ± 5.9 (1.61)	10.5 ± 6.5	11.7 ± 6.4 (1.83)	4.5 ± 2.5
Bellingshausen/ Amundsen	−8.3 ± 2.9 (***2.86***)	−5.4 ± 1.9	−4.1 ± 4.9 (0.84)	−1.9 ± 2.3	−9.6 ± 5.3 (1.81)	−5.3 ± 2.9	−12.5 ± 3.2 (***3.91***)	−14.8 ± 3.8	−7.0 ± 4.2 (1.67)	−5.2 ± 3.1

[a]Both are given as 10^3 km^2 a^{-1} and as % decade^{-1}. R is the ratio of the absolute value of the trend to its standard deviation. Assuming a null hypothesis of zero trend and 26 degrees of freedom, R values in bold indicate a statistical significance of 95%; values in italicized bold indicate a significance level of 99%.

Over the 28 years, the September ice extents range from a maximum of 18.9 × 10^6 km^2 in 2006 to a minimum of 17.5 × 10^6 km^2 in 1986. The February ice extents range from a maximum of 3.75 × 10^6 km^2 in 2003 to a minimum of 2.46 × 10^6 km^2 in 1993. When the record ran only through 1998, the maximum September extent (18.7 × 10^6 km^2) had been in 1998 [*Zwally et al.*, 2002]. The 2006 September extent of 18.9 × 10^6 km^2 is 0.19 × 10^6 km^2 greater than the value for 1998, but is well within one standard deviation of the 28-year mean. The minimum February extent has not changed. Interestingly, 2006 had the third lowest February extent, in addition to the highest September extent.

[9] The monthly deviations show large fluctuations from year to year, but with markedly smaller amplitudes from 1989 up to 1993 (Figure 3b). The overall trend is positive at 11,100 ± 2,600 km^2 a^{-1} (R = 4.25) which is slightly less than the 20-year (1979–1998) trend of 11,200 ± 4,200 km^2 a^{-1} (R = 2.67) reported previously [*Zwally et al.*, 2002], but the increase in the value of R over the two periods is considerable, resulting in a 99% level of statistical significance for the 28-year trend.

[10] The yearly and seasonally averaged extents all show positive trends (Figure 3c). The yearly trend in sea ice extents is 11,500 ± 4,600 km^2 a^{-1} (Table 1). This trend is somewhat greater than the value 11,000 ± 7,000 km^2 a^{-1} reported previously for the 20-year period 1978–1998 [*Zwally et al.*, 2002] and is statistically significant at the 95% level (Table 1). On a seasonal basis autumn shows the largest positive km^2 a^{-1} trend followed by the winter trend. The spring and summer trends are about half those for autumn (Table 1).

3.1.2. Weddell Sea

[11] The Weddell Sea sector is the largest of the five sectors and also has the largest sea ice cover. The phasing of the annual cycle of sea ice extent is similar to that of the Southern Hemisphere total, including minimum ice cover in February and maximum ice cover in September. Most of the sea ice remaining in February is found eastward of the Antarctic Peninsula (Figure 1). There is considerable interannual variability, which is particularly evident in the annual maxima and minima (Figure 4a). The annual minimum Weddell Sea ice extent for the 28-year period ranged from 0.835 × 10^6 km^2 in February 1988 to 1.84 × 10^6 km^2 in February 2003, whereas the annual maximum Weddell Sea ice extent ranged from 6.00 × 10^6 km^2 in September 1990 to 7.60 × 10^6 km^2 in September 1980.

[12] The Weddell Sea ice extent monthly deviations for the 28-year period show large excursions of up to nearly one million km^2 about the trend line (Figure 4b). The trend line itself has a positive slope at 3,300 ± 2,300 km^2 a^{-1} but is considerably smaller than the corresponding trend of 5,900 ± 3,600 km^2 a^{-1} reported previously for the 20-year period 1979–1998 [*Zwally et al.*, 2002].

[13] The yearly trend is positive with close to the same magnitude as the trend for the monthly deviations (Table 1 versus Figure 4b), whereas the seasonal trends differ in sign (Figure 4c). Both the winter and spring trends are negative, and the summer and autumn trends are positive (Table 1). The positive summer trend is more than an order of magnitude larger than the negative winter and spring trends. The signs of the trends are the same as those observed

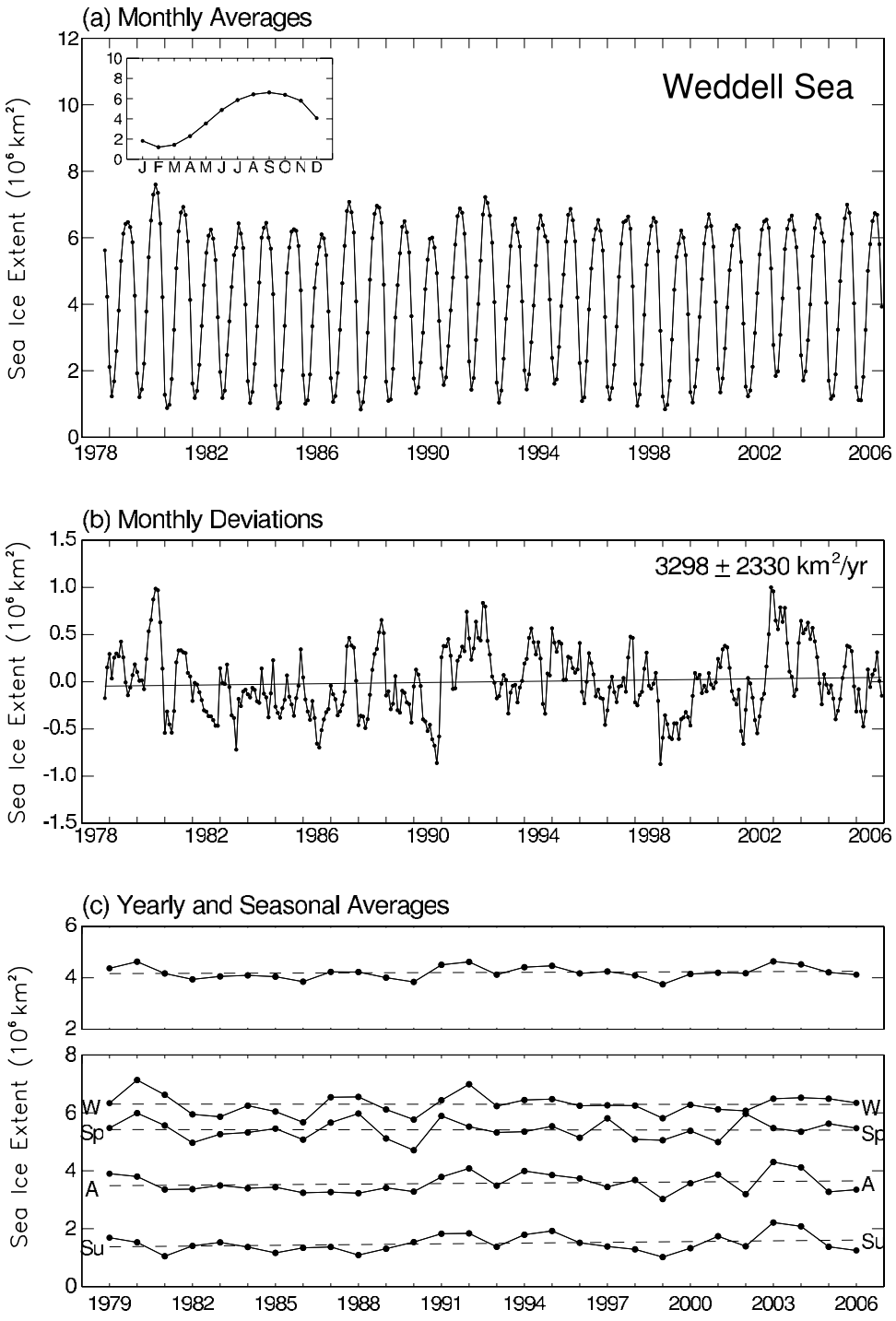

Figure 4. Time series of sea ice extent for the Weddell Sea sector, similar to Figure 3.

earlier for the 20-year period [*Zwally et al.*, 2002]. The largest difference between the two sets of results occurs for the spring season, for which the negative trend for the 28-year period is more than a factor of eight smaller in magnitude than for the 20-year period.

3.1.3. Indian Ocean

[14] The average annual cycle for the Indian Ocean has a winter peak in October rather than September, whereas the summer minimum is in February, as for each of the other sectors (Figure 5a, inset). This is true for both the 20- and 28-year periods. In comparison with the Weddell Sea, the Indian Ocean has much less ice, with the highest October maximum ice extent at 4.22×10^6 km^2 in October 2004. The Indian Ocean also shows less interannual variability compared with the Weddell Sea sector and almost no ice in summer (Figure 5a). The trend of the monthly deviations is 3,700 ± 1,200 km^2 a^{-1} (Figure 5b). This trend contrasts with the negative trend of −1,900 ± 1,800 km^2 a^{-1} reported

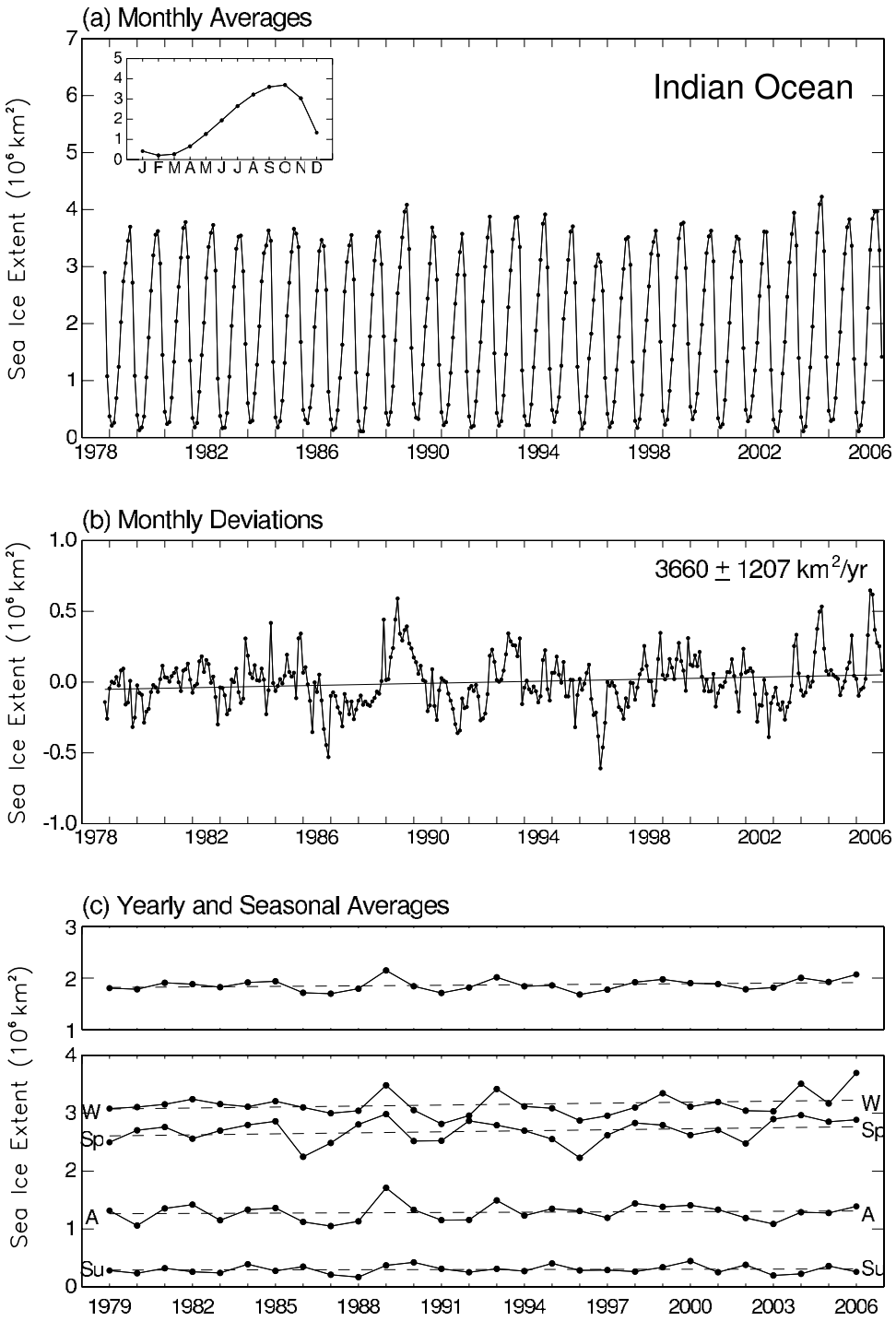

Figure 5. Time series of sea ice extent for the Indian Ocean sector, similar to Figure 3.

previously for the 20-year period 1979–1998 [*Zwally et al.*, 2002]. This reversal in sign resulted from the higher than average October sea ice extents in the last 4 years of the record, 2003–2006.

[15] The yearly and seasonal average trends are all positive (Figure 5c and Table 1), whereas the 20-year results show a negative yearly trend, negative trends for winter and spring, and positive trends for summer and autumn [*Zwally et al.*, 2002].

3.1.4. Western Pacific Ocean

[16] The western Pacific Ocean sector has less ice than the Indian Ocean sector, but has considerable interannual variability both in its winter maxima and summer minima. On average, the winter peak occurs in September, but is only slightly greater than its average October value (Figure 6a, inset). The sea ice extents for the winter months of July, August, and September range from 1.32×10^6 km^2 in July 2002 to 2.47×10^6 km^2 in September 1982

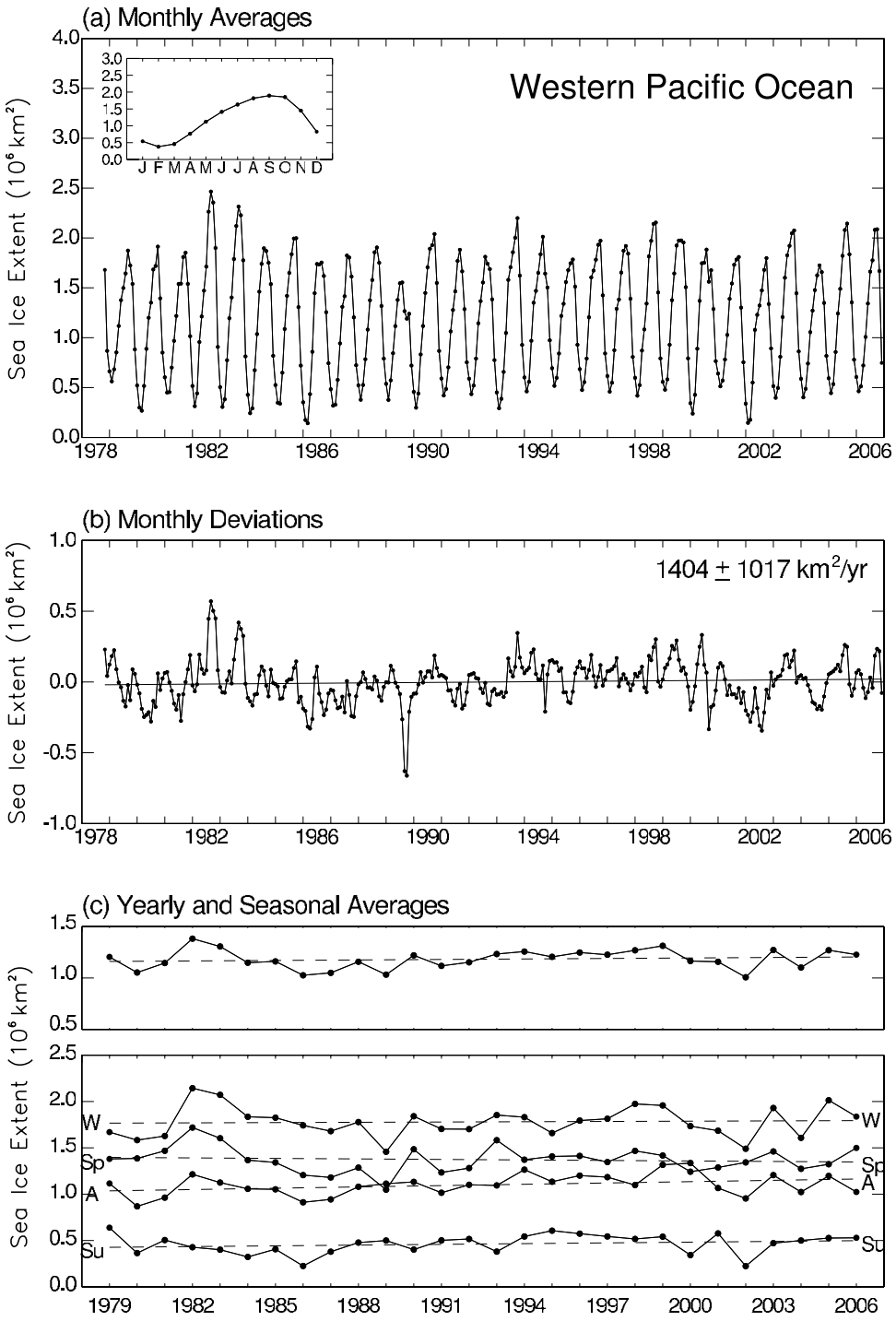

Figure 6. Time series of sea ice extent for the western Pacific Ocean sector, similar to Figure 3.

(Figure 6a). The ice extents for the summer months of January, February, and March range from a low of 0.143 × 10^6 km^2 in March 1986 to a high of 0.695 × 10^6 km^2 in January 1995.

[17] The monthly deviation trend of 1,400 ± 1,000 km^2 a^{-1} (Figure 6b) is less than the 2,300 ± 1,700 km^2 a^{-1} reported for the 20-year time series [*Zwally et al.*, 2002]. On a yearly basis the 28-year trend is less than half that of the 20-year trend. All of the 28-year seasonal trends are also less than for the corresponding 20-year trends. For both the 20- and 28-year periods, the seasonal trends are positive, except for spring.

3.1.5. Ross Sea

[18] The Ross Sea sector has a smaller overall ice cover than the Weddell Sea sector, but a greater interannual variability (Figure 7a). This is particularly noticeable in the summer minima ice extents. The Ross Sea exhibits a rather sharp minimum in February and a broader

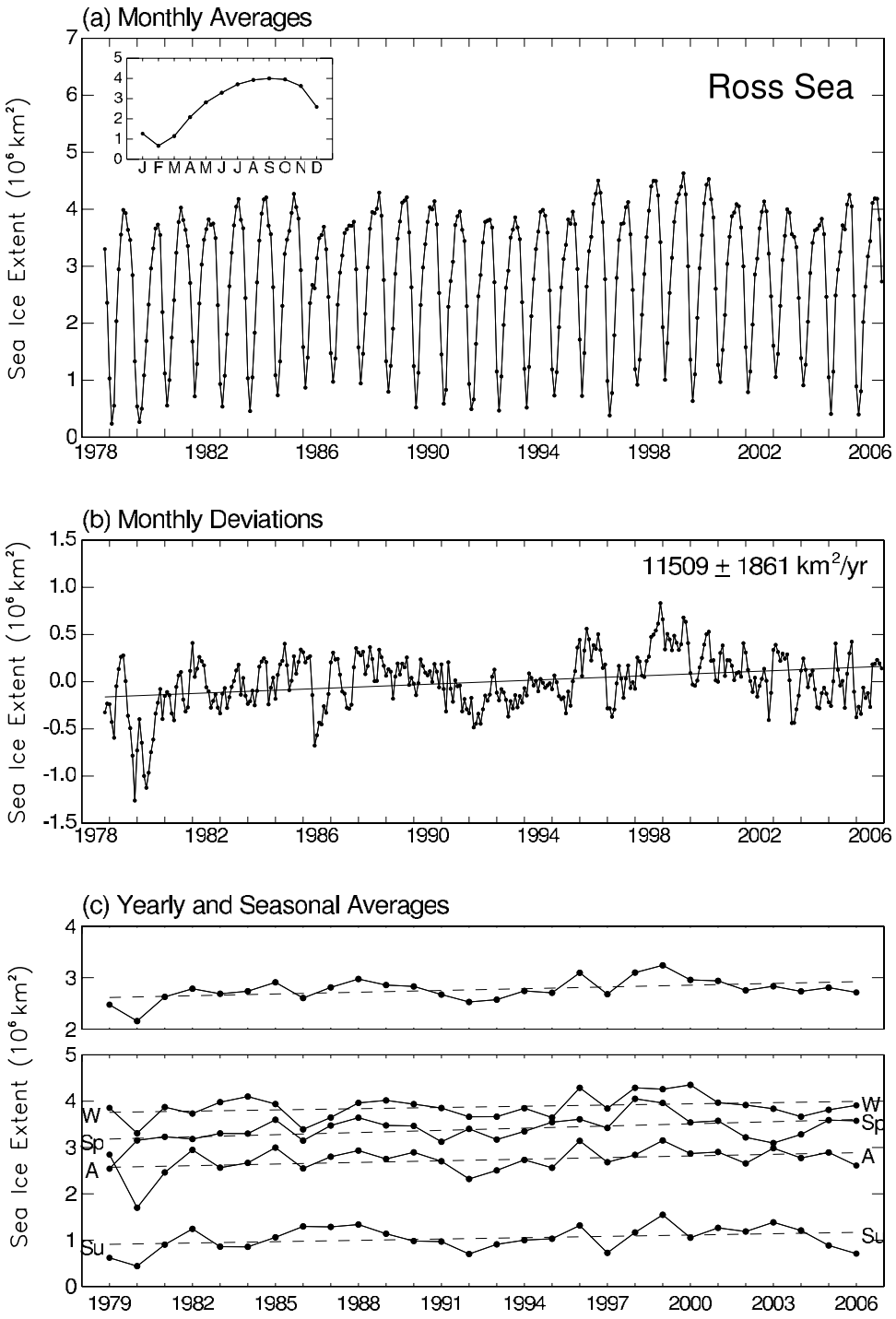

Figure 7. Time series of sea ice extent for the Ross Sea sector, similar to Figure 3.

autumn and winter maximum extent (Figure 7a, inset) than the overall annual cycle for the entire Southern Hemisphere. The February extents range from 0.237 × 10^6 km^2 in 1979 to 1.05 × 10^6 km^2 in 2003. The September extents range from 3.55 × 10^6 km^2 in 1986 to 4.53 × 10^6 km^2 in 2000, although the 28-year maximum sea ice extent of 4.63 × 10^6 km^2 occurs in October 1999 (Figure 7a).

[19] The 28-year monthly deviation trend (11,500 ± 1,900 km^2 a^{-1}) is more than 3 times that (3,300 ± 2,300 km^2 a^{-1}) for the Weddell Sea (Figure 4b), but is smaller than the corresponding 20-year trend (18,400 ± 3,000 km^2 a^{-1}) reported by *Zwally et al.* [2002]. For both the 20-year and 28-year periods, the seasonal trends are positive, but all are smaller for the 28-year period. The 28-year trend for spring is about half that of the 20-year

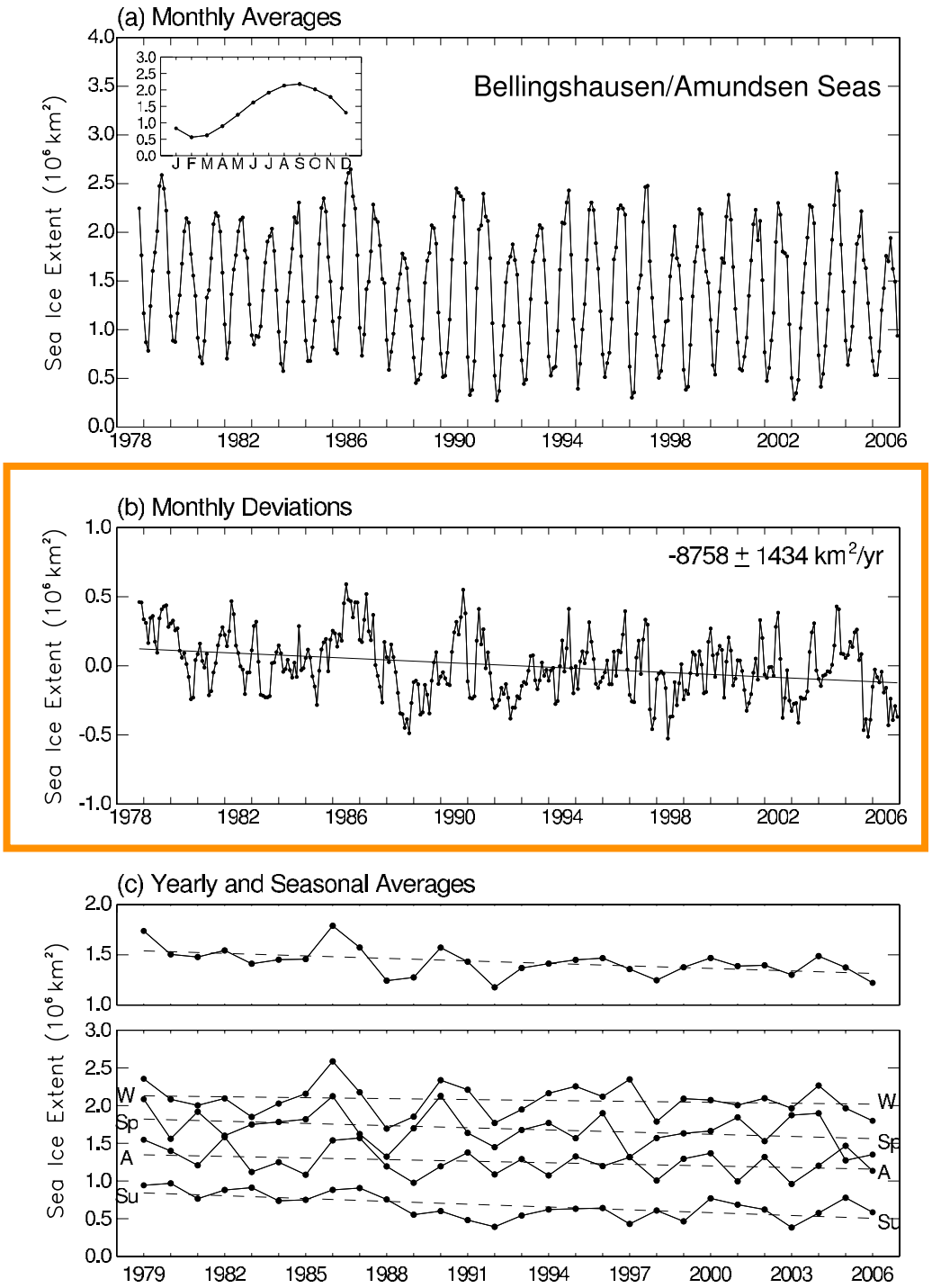

Figure 8. Time series of sea ice extent for the Bellingshausen/Amundsen seas sector, similar to Figure 3.

trend. Nonetheless, the yearly and spring trends for the 28-year record are both statistically significant at the 95% level (Table 1).

3.1.6. Bellingshausen/Amundsen Seas

[20] Since 1990 the amplitude of the seasonal sea ice cover in the Bellingshausen/Amundsen seas sector appears to have increased on average as a result of the smaller summer ice cover (Figure 8a). The maximum ice extent during the three summer months occurred in January 1979, whereas the minimum extent occurred in February 1992.

[21] The overall trend of the monthly deviations is $-8{,}800 \pm 1{,}400$ km^2 a^{-1} (Figure 8b) which is considerably less than the trend ($-14{,}100 \pm 2{,}200$ km^2 a^{-1}) obtained previously for the 20-year time series [*Zwally et al.*, 2002]. The Bellingshausen/Amundsen seas sector is now the only

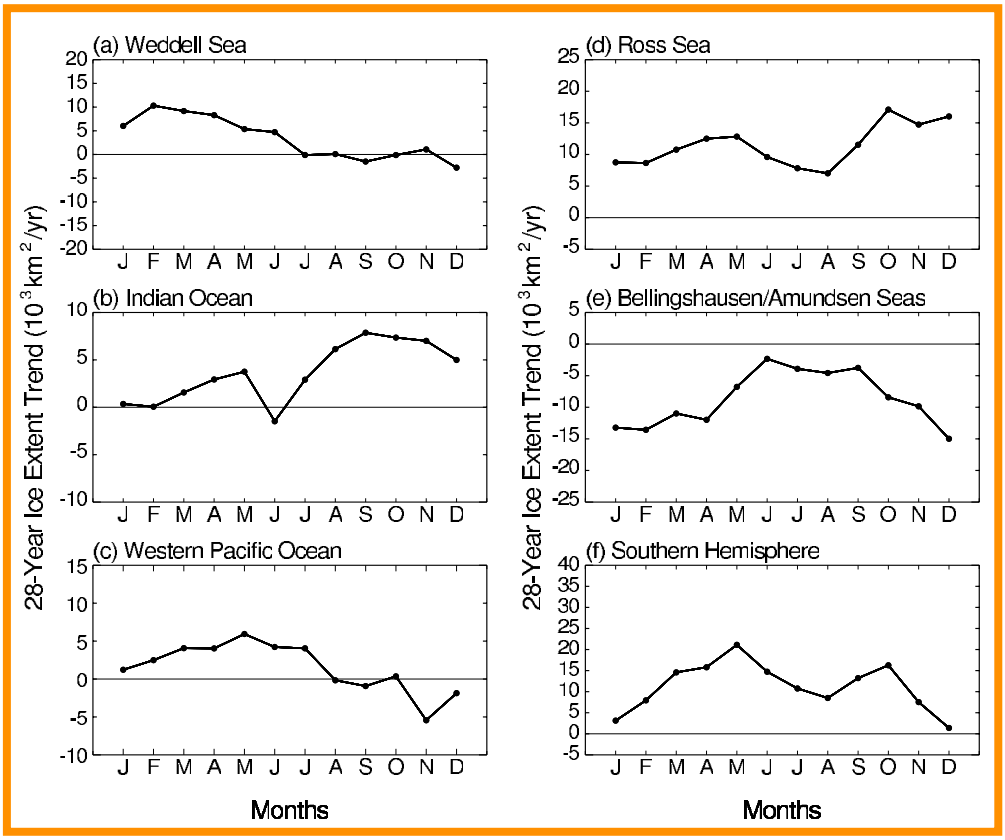

Figure 9. Twenty-eight-year sea ice extent trends by month for all five sectors and for the Southern Hemisphere.

sector with a negative monthly deviation trend, versus the 20-year record, for which the Indian Ocean also had a negative trend. The yearly and seasonal trends obtained here for the Bellingshausen/Amundsen seas (Figure 8c and Table 1) are less negative, except for winter, than the corresponding trends obtained for the 20-year time series [*Zwally et al.*, 2002]. Summer has the most negative trend, while winter has the least negative trend (Figure 8c). The 20-year trends show the same seasonal pattern. The Bellingshausen/Amundsen seas sector exhibits the two largest R values. These occur for the yearly trend (R = 2.86) and the summer trend (R = 3.91). Both are significant at the 99% level (Table 1).

3.1.7. Sea Ice Extent Trends by Month for All Regions

[22] Sea ice extent trends by month based on the 28-year record for all five sectors and for the Southern Hemisphere as a whole are presented in Figure 9. The most striking feature of Figure 9 is how different the monthly trend patterns are for each of the five sectors. The Weddell Sea and western Pacific Ocean sectors have mostly positive trends with the largest positive values occurring during the first half of the year. In contrast, the Indian Ocean sector, which also has mostly positive trends, has its largest values during the last half of the year. The Ross Sea sector has positive trends for all 12 months of the year and for most months exhibits the largest positive trends of all five sectors. The Bellingshausen/Amundsen seas sector has negative trends for each of the 12 months, with the largest negative trend occurring in December and the next two largest negative trends occurring in February and January. For the Southern Hemisphere as a whole all 12 months exhibit positive trends, with the smallest trend occurring in December and the largest trend occurring in May.

3.2. Sea Ice Areas

[23] The sea ice area for a given region is defined as the sum of the products of ice concentration and pixel area for each pixel within the region of interest. The sea ice area time series are generally similar to those of sea ice extent except that the ice area magnitudes are always smaller (Figures 10–15). For the Southern Hemisphere as a whole the month of minimum ice area is February whereas the month of maximum ice area is September (Figure 10a, inset), both identical to the phasing for ice extent. The Southern Hemisphere monthly deviation trend for ice area (Figure 10b) is smaller than that for the ice extent (Figure 3b). The 28-year monthly deviation trend for ice area of 9,600 ± 2,400 km^2 a^{-1} is less than the corresponding 20-year trend of 10,900 ± 3,700 km^2 a^{-1} [*Zwally et al.*, 2002]. Seasonally, the ice area trends are smaller than the ice extent trends for winter and spring, but the area trend is larger for autumn (Tables 1 and 2).

[24] Regionally, the yearly ice area trends in km^2 a^{-1} all have the same sign as the ice extent trends, but are smaller in magnitude, except for the western Pacific Ocean sector (Tables 1 and 2). This implies that the ice cover of this sector is becoming more compact, whereas the ice covers of the other sectors with positive trends are becoming less compact.

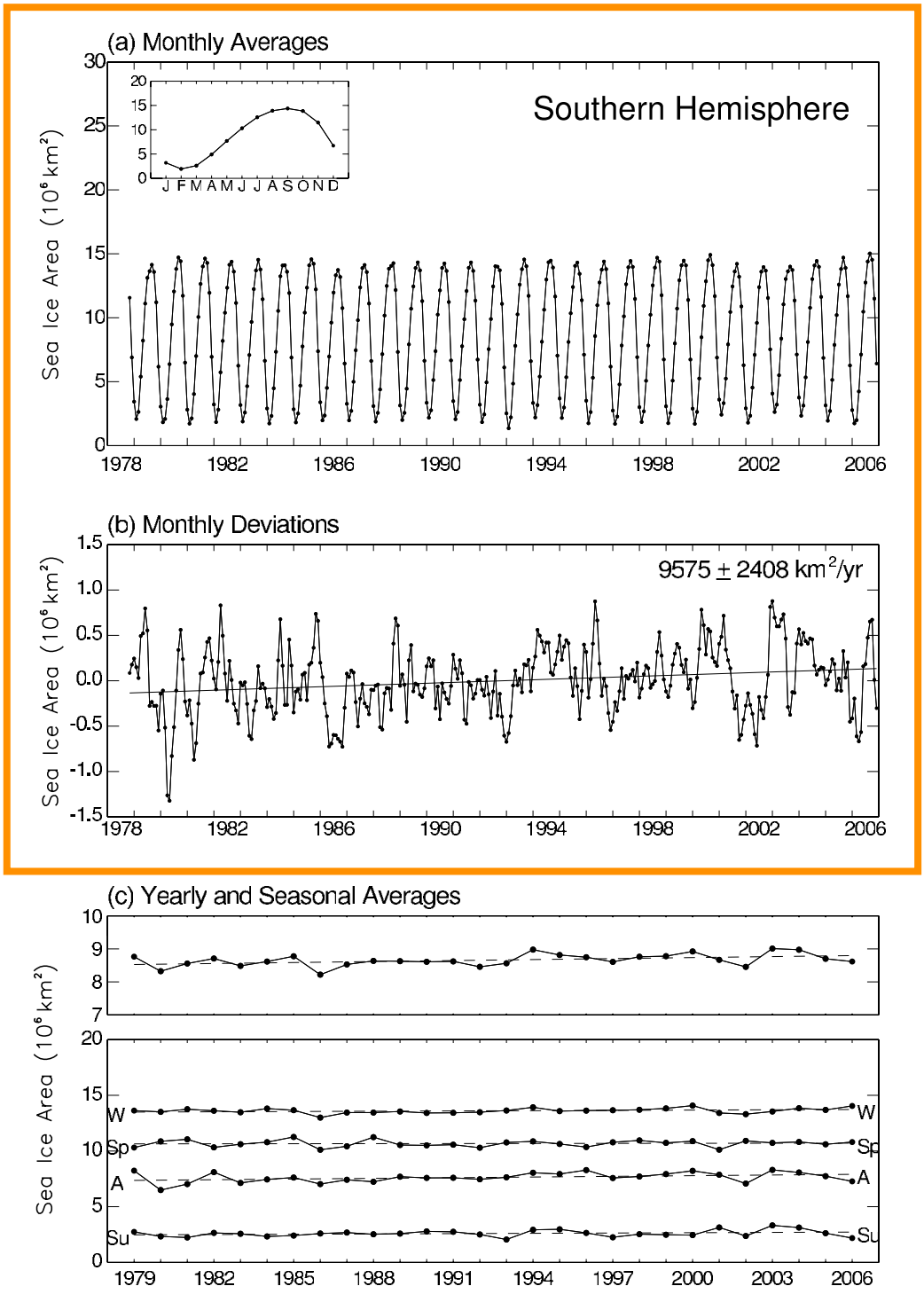

Figure 10. Time series of (a) monthly averages of sea ice area for the Southern Hemisphere from November 1978 through December 2006. The inset shows the annual cycle computed from the 28 years of data. (b) Monthly deviations of sea ice area fitted with a linear least squares best fit trend line. (c) Yearly and seasonal averages of sea ice areas with linear least squares best fit trend line. Summer averages (Su) are for January–March, autumn averages (A) are for April–June, winter averages (W) are for July–September, and spring averages (Sp) are for October–December.

[25] On a seasonal basis, the signs of the ice area trends match those of the ice extents, but are not consistently smaller than the ice extent trends. The Weddell Sea sector ice area trends are larger in magnitude than the ice extent trends in winter and spring, whereas the western Pacific Ocean sector has larger ice area than ice extent trends for winter, summer, and autumn (Tables 1 and 2).

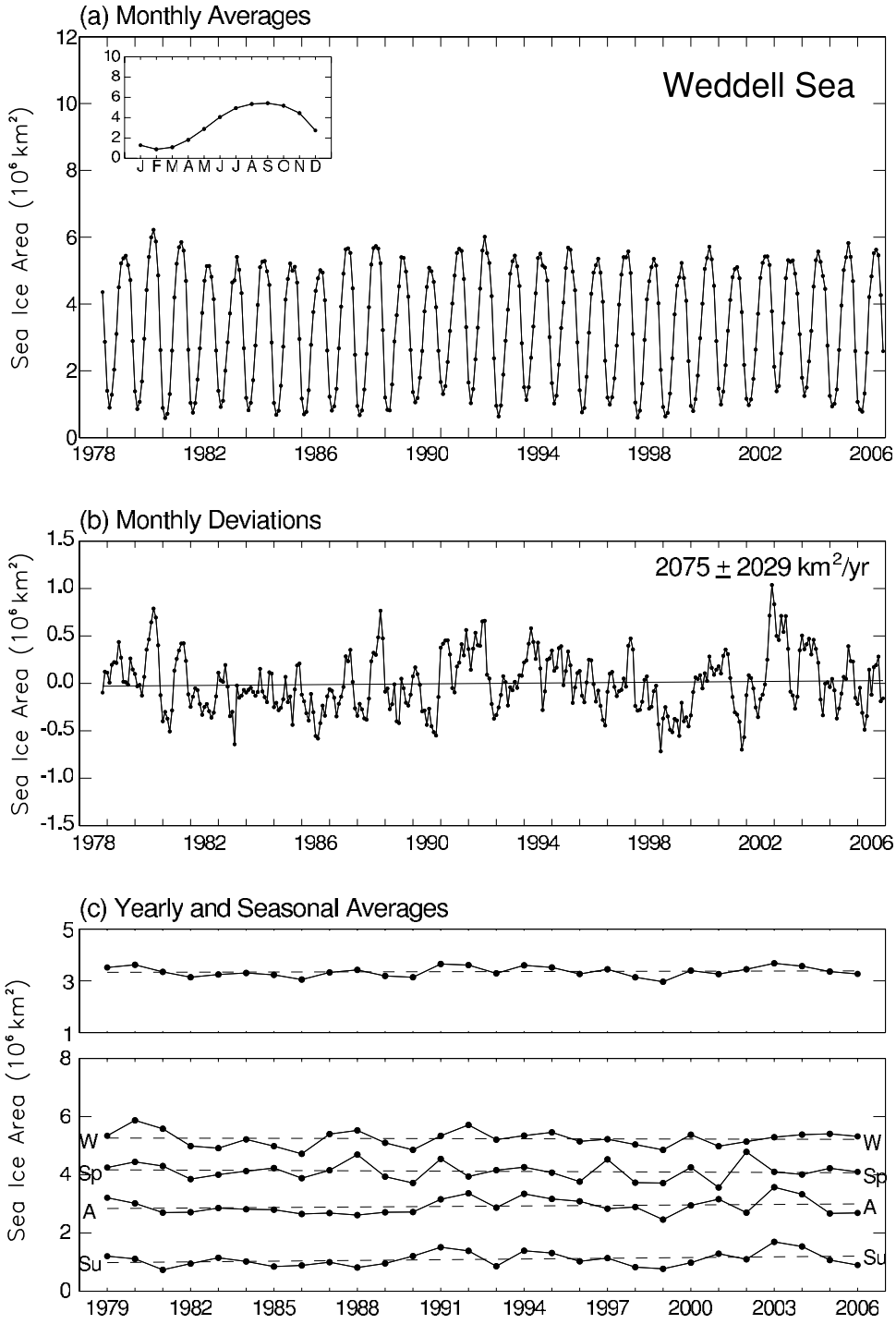

Figure 11. Time series of sea ice area for the Weddell Sea sector, similar to Figure 10.

[26] The seasonal pattern of ice area trends is similar to that of the ice extent trends, but the ice area trends are mostly smaller in magnitude (Figures 9 and 16). Other differences include negative ice area trends for the Weddell Sea sector August through December instead of just for September and December and a very small positive ice area trend in June for the Bellingshausen/Amundsen seas sector. For the Southern Hemisphere as a whole, the ice area trend is negative for November in contrast to the 12 months of positive ice extent trends.

[27] Comparison of the 20-year and 28-year monthly deviation ice area trends reveals that for the Southern Hemisphere as a whole and for each sector except for the Indian Ocean the ice area trends are smaller for the 28-year period and of the same sign. The Indian Ocean sector trend

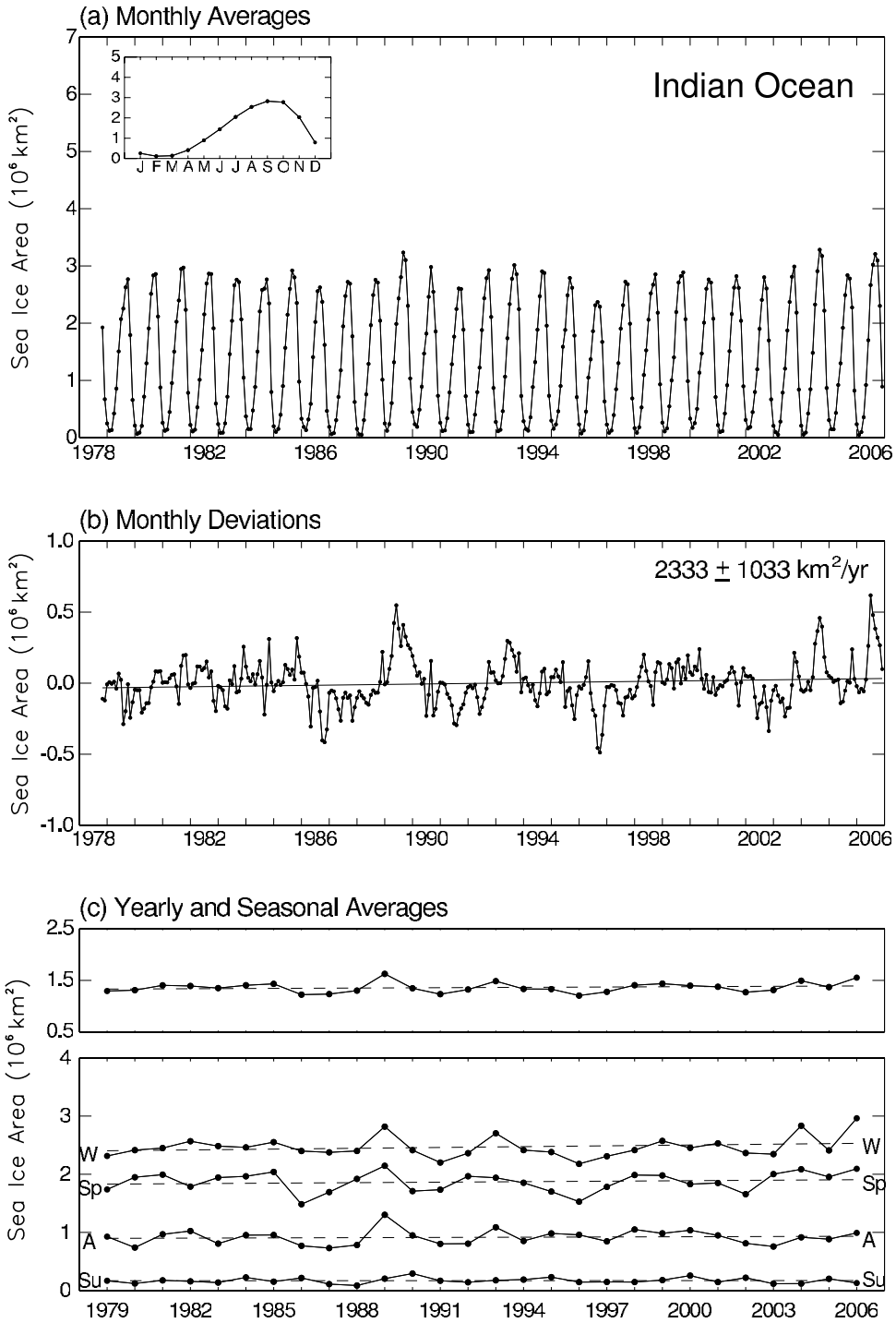

Figure 12. Time series of sea ice area for the Indian Ocean sector, similar to Figure 10.

reverses sign from −2,600 ± 1,500 km^2 a^{-1} for the 20-year period to 2,300 ± 1,000 km^2 a^{-1} for the 28-year period. A similar reversal in sign also occurred for the ice extent trend for this sector.

4. Discussion and Conclusions

[28] This study extends the analyses of the sea ice time series reported by *Zwally et al.* [2002] from 20 years (1979–1998) to 28 years (1979–2006). A summary of the yearly trends of sea ice extent for both the 20- and 28-year periods is presented in Table 3. The eight additional years have revealed some significant changes. The total Antarctic sea ice extent increased its yearly trend during the two periods from 11,000 ± 7,000 km^2 a^{-1} (0.96 ± 0.61% decade^{-1}) to 11,500 ± 4,600 km^2 a^{-1} (1.0 ± 0.4% decade^{-1}) and is statistically significant at a level of 95%. This increase reflects contrasting changes in the sector trends.

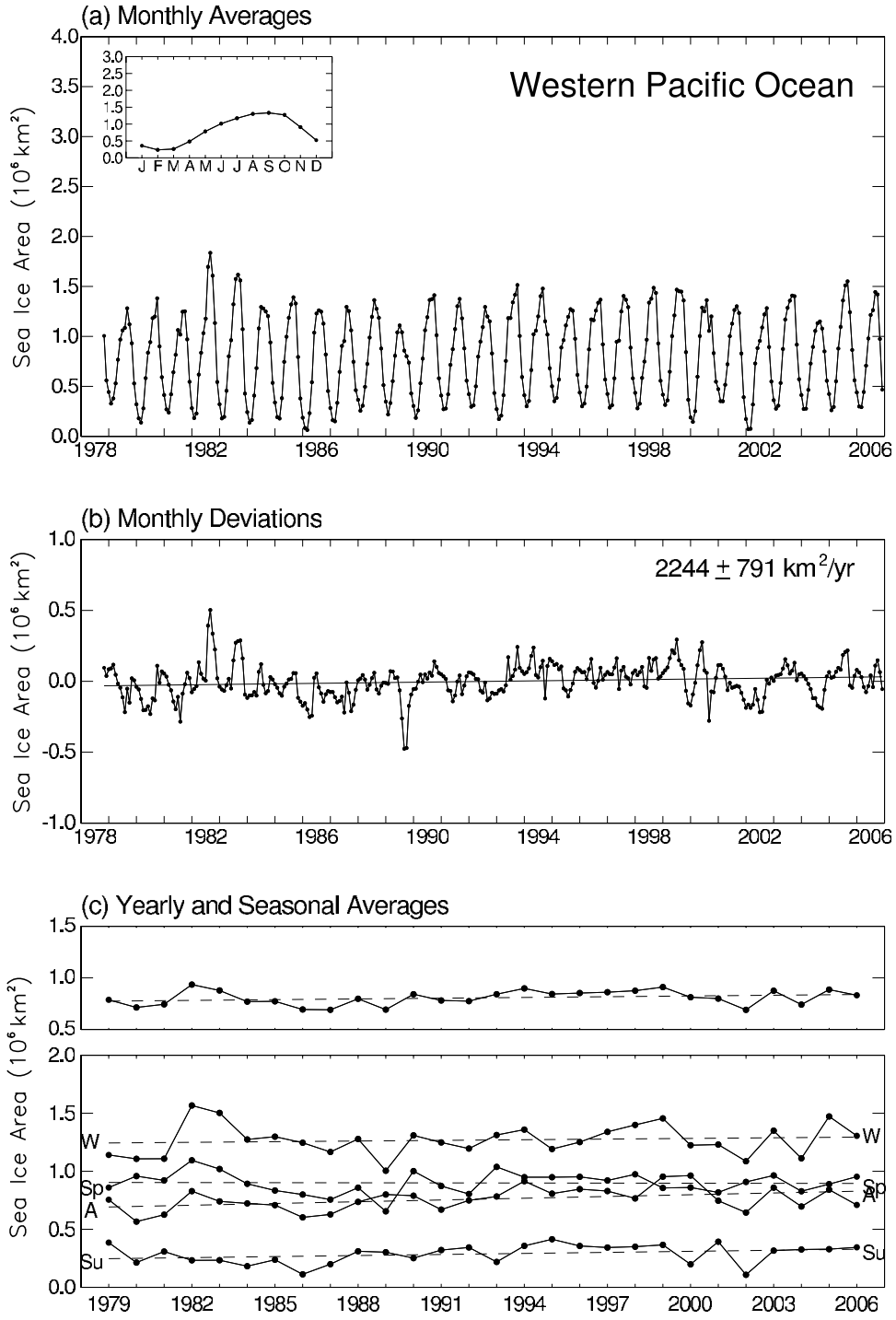

Figure 13. Time series of sea ice area for the western Pacific Ocean sector, similar to Figure 10.

[29] For the Weddell Sea, western Pacific Ocean, and Ross Sea sectors there are now smaller positive yearly trends of sea ice extents than for the 20-year record, whereas for the Bellingshausen/Amundsen seas sector there is a weakening of its negative trend, but with an increase in its level of statistical significance (Table 3). In contrast, the Indian Ocean sector shows a shift from a negative trend to a positive trend between the two periods, but neither trend is statistically significant. A somewhat similar pattern of yearly trend changes between the two periods is apparent in the sea ice area time series with the exception that there is now, for the 28-year record, a slightly smaller trend for the Southern Hemisphere as a whole and a slightly larger trend for the Weddell Sea sector (Table 3).

[30] On a seasonal basis, going from the 20- to 28-year period, there was a lessening of the negative sea ice extent trend for the Bellingshausen/Amundsen seas sector for

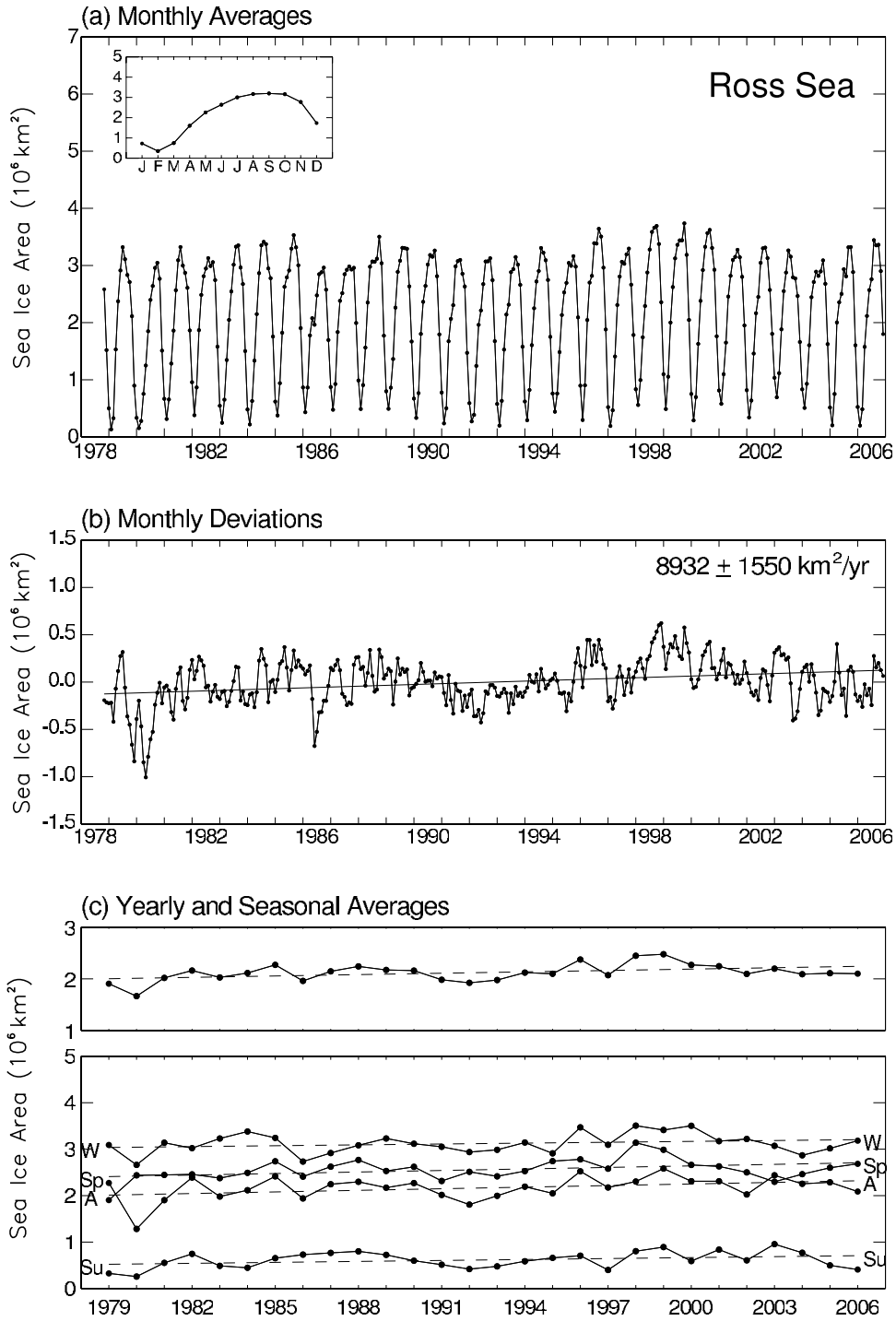

Figure 14. Time series of sea ice area for the Ross Sea sector, similar to Figure 10.

summer and autumn, whereas the sign reversal for the Indian Ocean sector trends occurred in winter and spring only. For the Weddell Sea, western Pacific Ocean, and Ross Sea sectors there was a reduction in the magnitude of the trends in all seasons, although the sign of the trend differed with season.

[31] An examination of Table 3 shows that the only two sectors exhibiting statistically significant trends in the yearly averages both for the 20-year and 28-year periods are the Ross Sea and the Bellingshausen/Amundsen seas sectors. The eight additional years do not produce any new sectors with trends significant at the 95% level, although the R values for the Weddell and Indian sector trends increased and the western Pacific R value decreased. On a % decade^{-1} basis, the Ross Sea positive ice extent trend decreased from 6.5 ± 2.8% decade^{-1} to 4.4 ± 1.7% decade^{-1}, and the Bellingshausen/Amundsen seas negative trend also decreased in magnitude from −9.2 ± 3.6%

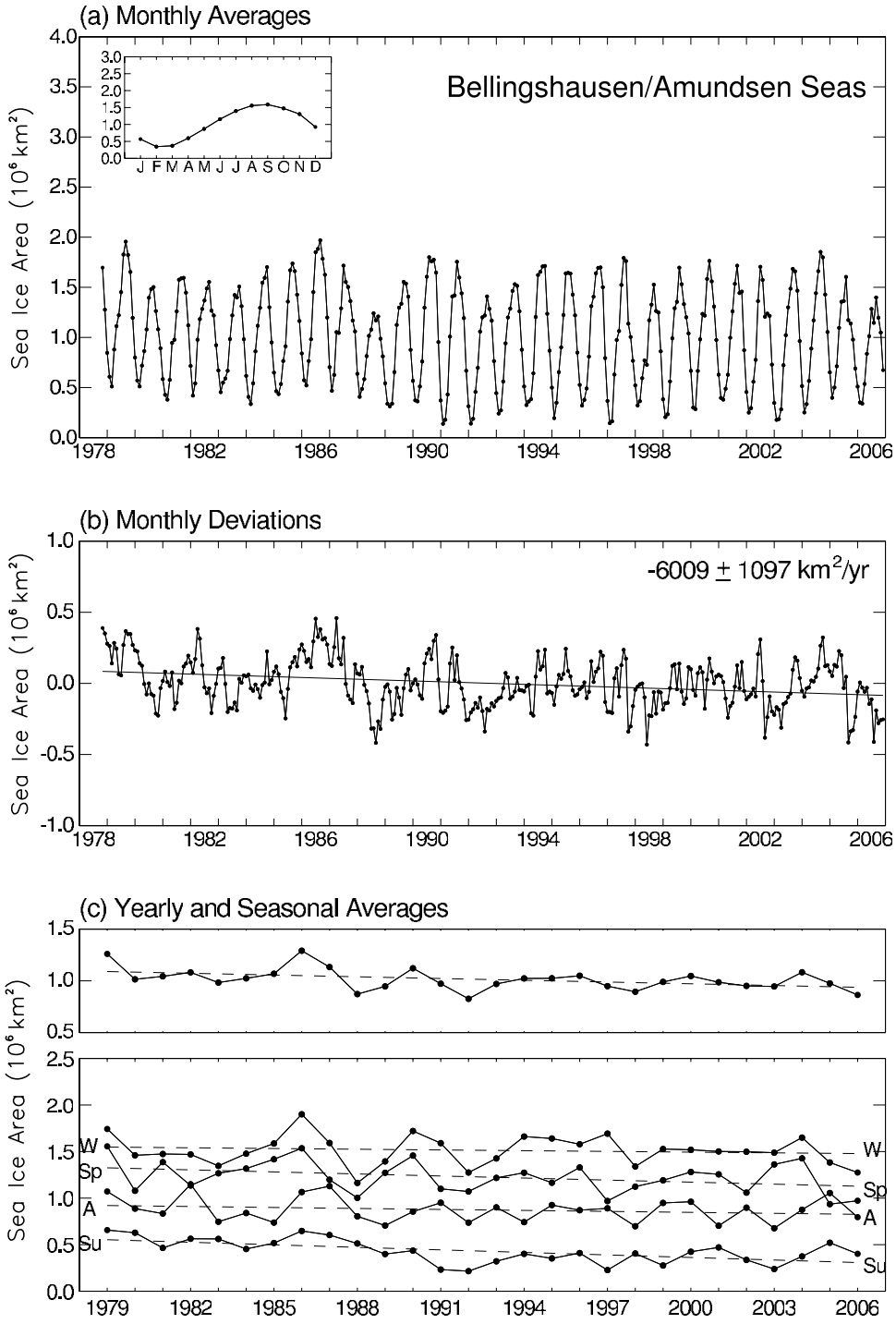

Figure 15. Time series of sea ice area for the Bellingshausen/Amundsen seas sector, similar to Figure 10.

decade^{-1} to $-5.4 \pm 1.9\%$ decade^{-1}. None of the other sectors exhibit significant ice extent trends (R values are all less than 1.4) for either period.

[32] The weakening of the positive trends for the Weddell, western Pacific, and Ross Sea sectors, the corresponding weakening of the negative trend in the Bellingshausen/Amundsen seas sector, and the reversal from a negative to positive trend in the Indian Ocean sector suggest that changes might have occurred in the large-scale atmospheric forcing over the intervening 8-year period. What atmospheric changes could have resulted in the observed change in trends?

[33] Previous studies have demonstrated an association between ENSO and the retreat of the ice cover in the Bellingshausen/Amundsen seas sector. In particular, *Kwok and Comiso* [2002] showed a strong association during each

Table 2. Yearly and Seasonal Antarctic Sea Ice Area Trends for the Period 1979–2006 With Estimated Standard Deviations[a]

Sector	Yearly		Winter (JAS)		Spring (OND)		Summer (JFM)		Autumn (AMJ)	
	10^3 km^2 a^{-1} (R)	Percent Decade^{-1}	10^3 km^2 a^{-1} (R)	Percent Decade^{-1}	10^3 km^2 a^{-1} (R)	Percent Decade^{-1}	10^3 km^2 a^{-1} (R)	Percent Decade^{-1}	10^3 km^2 a^{-1} (R)	Percent Decade^{-1}
SH	10.0 ± 4.0 (**2.50**)	1.2 ± 0.5	8.5 ± 5.1 (1.67)	0.6 ± 0.4	2.4 ± 7.1 (0.34)	0.2 ± 0.7	9.1 ± 6.9 (1.32)	3.7 ± 2.8	20.2 ± 9.9 (2.04)	2.7 ± 1.3
Weddell	2.1 ± 4.5 (0.47)	0.6 ± 1.4	−1.7 ± 6.4 (0.27)	−0.3 ± 1.2	−3.8 ± 7.2 (0.53)	−0.9 ± 1.7	8.2 ± 5.7 (1.44)	8.4 ± 5.8	5.9 ± 6.5 (0.91)	2.1 ± 2.3
Indian	2.2 ± 2.3 (0.96)	1.7 ± 1.7	4.7 ± 4.2 (1.12)	2.0 ± 1.7	2.8 ± 3.9 (0.72)	1.5 ± 2.2	0.1 ± 1.1 (0.09)	0.7 ± 6.7	1.3 ± 3.0 (0.43)	1.5 ± 3.4
W. Pacific	2.4 ± 1.7 (1.41)	3.1 ± 2.1	1.9 ± 3.2 (0.59)	1.5 ± 2.6	−0.3 ± 2.2 (0.14)	−0.3 ± 2.4	3.0 ± 1.9 (1.58)	12.2 ± 7.6	5.0 ± 2.2 (**2.27**)	7.3 ± 3.2
Ross	8.9 ± 3.6 (**2.47**)	4.4 ± 1.8	6.2 ± 4.9 (1.27)	2.1 ± 1.6	11.0 ± 5.0 (**2.20**)	4.6 ± 2.1	6.8 ± 4.0 (1.70)	13.1 ± 7.7	11.4 ± 5.7 (2.00)	5.7 ± 2.8
Bellingshausen/ Amundsen	−5.6 ± 2.2 (**2.55**)	−5.2 ± 2.1	−2.6 ± 3.8 (0.68)	−1.7 ± 2.5	−7.3 ± 3.8 (1.92)	−5.5 ± 2.9	−9.1 ± 2.5 (***3.64***)	−16.4 ± 4.5	−3.5 ± 3.1 (1.13)	−3.8 ± 3.4

[a]Both are given as 10^3 km^2 a^{-1} and as % decade^{-1}. R is the ratio of the absolute value of the trend to its standard deviation. Assuming a null hypothesis of zero trend and 26 degrees of freedom, R values in bold indicate a statistical significance of 95%; values in italicized bold indicate a significance level of 99%.

of the four episodes of negative Southern Oscillation Index (SOI) and the retreat of the ice cover for the period 1982–1998. Since 1998 the SOI has been in a more neutral phase (average index −0.04 for the period 1999–2006 versus −0.4 for the period 1982–1998) which may help explain the reduction in the rate of sea ice retreat in the Bellingshausen/Amundsen seas sector and the lessening of the positive trend in the Weddell Sea sector, but not the lessening of the positive trend in the Ross Sea sector.

[34] The opposing changes in the Bellingshausen/Amundsen seas and Indian Ocean sectors relative to the other sectors suggest the possible influence of an atmospheric zonal wave 2 pattern. Whether these changes have resulted from the action of the Antarctic Circumpolar Wave (ACW) [*White and Peterson*, 1996] is not obvious given that the propagation pattern of the ACW has a period of about 8 years and is discontinuous in the Indian Ocean sector [*Yuan and Martinson*, 2000]. Thus, the atmospheric influence may involve another mode of variability or a combination of modes.

[35] In a study of low-frequency variability in Southern Hemisphere atmospheric circulation, *Carleton* [2003] finds several dominant modes of variability. There is a zonally symmetric mode, the Antarctic Oscillation, but also zonally asymmetric modes represented by zonal wave numbers 1, 2, and 3. The wave 1 mode appears as an oscillation in pressure between the Weddell and east Antarctic sectors, whereas the wave 2 mode is strongest in the Pacific and southwest Atlantic sectors, which may be the result of the influence of ENSO [*Carleton*, 2003], and manifests itself as the ACW observed in the ice-ocean-atmosphere system [*White and Peterson*, 1996]. It has also been argued that the ACW may be a combination of zonal wave numbers 2 and 3 each having different spatial and temporal characteristics [*Venegas*, 2003]. The importance of the ACW in Antarctic atmospheric and oceanic interannual variability has also been questioned. An analysis of climate variables found that the eastward propagating wave explained only about 25% of the variability, its amplitude rapidly dissipated, and it was unable to complete its entire circumpolar journey [*Park et al.*, 2004].

[36] More recently, the influence of atmospheric zonal wave 3 on Antarctic sea ice variability has been examined [*Raphael*, 2007]. The sectors that show a positive correlation between wave 3 and sea ice variability are the Ross and Weddell seas and north of the Amery ice shelf (middle of our Indian Ocean sector) particularly during the autumn and winter months. Unfortunately, there is no clear wave 3 pattern in the changes observed here in either the ice extent trends or the changes observed in the trends between the 20- and 28-year periods.

[37] The fact that the ice extent trends for the Weddell, Indian, and western Pacific sectors are not particularly significant (none have R values greater than 1.35) may explain why the zonal wave patterns do not provide a consistent explanation. The degree to which trend significance plays a role here is unknown, but one would expect that the stronger the signal the easier it would be to find an association.

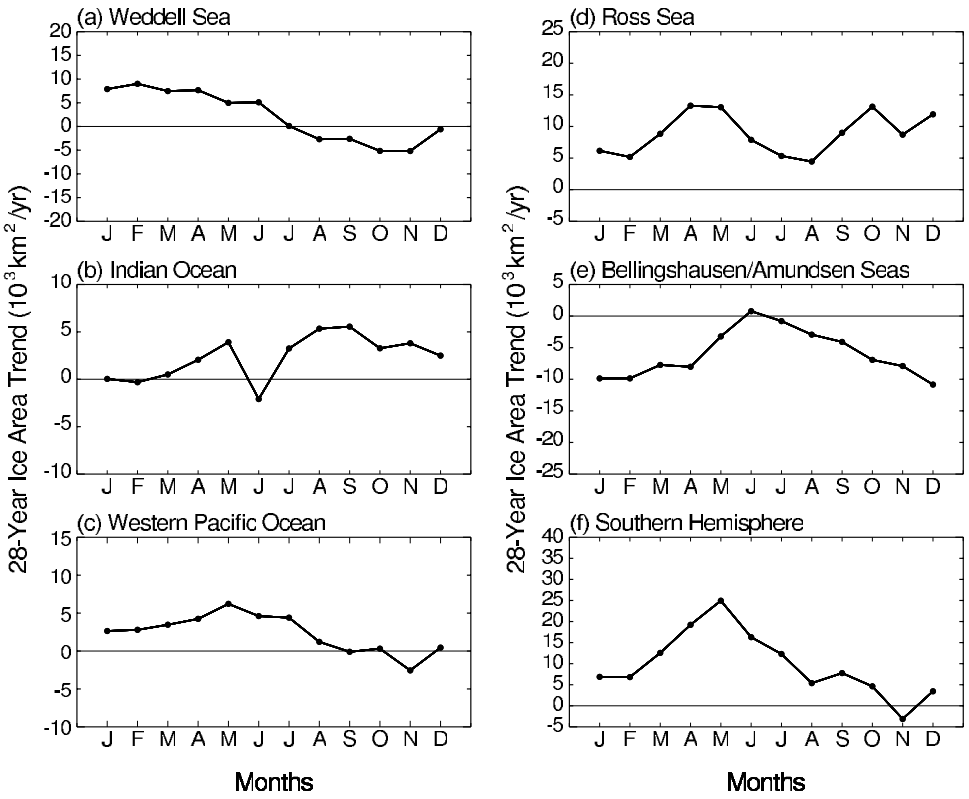

Figure 16. Twenty-eight-year sea ice area trends by month for all five sectors and for the Southern Hemisphere.

[38] Finally, the question of why the Southern Ocean as a whole has an increasing ice cover under warming atmospheric and oceanic conditions has been addressed by *Zhang* [2007] on the basis of a modeling study. The suggested mechanism involves reduced convective overturning in the ocean beneath the ice and hence reduced ocean heat flux available to melt ice, resulting in an overall increase in ice extent and volume. This, though, does not explain the regional differences observed, and thus the question of what is driving the observed changes remains unanswered, and the physical mechanisms explaining these changes remain to be determined.

[39] **Acknowledgments.** We thank Harry Stern, the Associate Editor, and two anonymous reviewers for their very helpful comments. We also thank Al Ivanoff and Nick DiGirolamo of Science Systems and Applications, Incorporated, for their help with processing the data and in generating the figures. The National Snow and Ice Data Center provided the DMSP F13 gridded brightness temperatures used for extending our sea ice concentration time series. This work was supported by NASA's Cryospheric Sciences Program and by NASA's Earth Observing System.

Table 3. Yearly Trends of Sea Ice Extent and Sea Ice Area for Both the 20-Year Period Previously Studied [*Zwally et al.*, 2002] and the 28-Year Period Reported Here[a]

	Sea Ice Extent 20-Year Trend		Sea Ice Extent 28-Year Trend		Sea Ice Area 20-Year Trend		Sea Ice Area 28-Year Trend	
Sector	10^3 km^2 a^{-1} (R)	Percent Decade^{-1}	10^3 km^2 a^{-1} (R)	Percent Decade^{-1}	10^3 km^2 a^{-1} (R)	Percent Decade^{-1}	10^3 km^2 a^{-1} (R)	Percent Decade^{-1}
SH	10.95 ± 6.95 (1.58)	0.96 ± 0.61	11.5 ± 4.6 (**2.50**)	1.0 ± 0.4	10.4 ± 6.4 (1.63)	1.2 ± 0.7	10.0 ± 4.0 (**2.50**)	1.2 ± 0.5
Weddell	3.9 ± 9.20 (0.42)	0.92 ± 2.19	3.3 ± 5.6 (0.59)	0.8 ± 1.4	1.6 ± 7.4 (0.22)	1.0 ± 2.2	2.1 ± 4.5 (0.47)	0.6 ± 1.4
Indian	−0.52 ± 4.51 (0.12)	−0.28 ± 2.45	3.5 ± 2.6 (1.35)	1.9 ± 1.4	−1.3 ± 3.9 (0.33)	−9.4 ± 2.9	2.2 ± 2.3 (0.96)	1.7 ± 1.7
W. Pacific	3.30 ± 3.68 (0.90)	3.13 ± 3.14	1.6 ± 2.2 (0.73)	1.4 ± 1.9	4.7 ± 2.7 (1.74)	5.9 ± 3.3	2.4 ± 1.7 (1.41)	3.1 ± 2.1
Ross	17.60 ± 7.56 (**2.33**)	6.45 ± 2.77	11.4 ± 4.6 (**2.48**)	4.4 ± 1.7	14.4 ± 6.1 (**2.36**)	6.9 ± 2.9	8.9 ± 3.6 (**2.47**)	4.4 ± 1.8
Bellingshausen/ Amundsen	−13.29 ± 5.26 (**2.53**)	−9.18 ± 3.63	−8.3 ± 2.9 (***2.86***)	−5.4 ± 1.9	−9.0 ± 4.1 (**2.20**)	−8.8 ± 4.0	−5.6 ± 2.2 (**2.55**)	−5.2 ± 2.1

[a]Both are given as 10^3 km^2 a^{-1} and as % decade^{-1}. R is the ratio of the absolute value of the trend to its standard deviation. Assuming a null hypothesis of zero trend and 26 degrees of freedom, R values in bold indicate a statistical significance of 95%; values in italicized bold indicate a significance level of 99%.

References

Carleton, A. M. (2003), Atmospheric teleconnections involving the Southern Ocean, *J. Geophys. Res.*, *108*(C4), 8080, doi:10.1029/2000JC000379.

Cavalieri, D. J., P. Gloersen, C. L. Parkinson, J. C. Comiso, and H. J. Zwally (1997), Observed hemispheric asymmetry in global sea ice changes, *Science*, *272*, 1104–1106, doi:10.1126/science.278.5340.1104.

Cavalieri, D. J., C. L. Parkinson, P. Gloersen, J. C. Comiso, and H. J. Zwally (1999), Deriving long-term time series of sea ice cover from satellite passive-microwave multisensor data sets, *J. Geophys. Res.*, *104*, 15803–15814, doi:10.1029/1999JC900081.

Cavalieri, D. J., C. L. Parkinson, and K. Y. Vinnikov (2003), 30-Year satellite record reveals contrasting Arctic and Antarctic decadal sea ice variability, *Geophys. Res. Lett.*, *30*(18), 1970, doi:10.1029/2003GL018031.

Kwok, R., and J. C. Comiso (2002), Southern Ocean climate and sea ice anomalies associated with the Southern Oscillation, *J. Clim.*, *15*, 487–501, doi:10.1175/1520-0442(2002)015<0487:SOCASI>2.0.CO;2.

Nicholls, N. (2001), Commentary and analysis: The insignificance of significance testing, *Bull. Am. Meteorol. Soc.*, *82*(5), 981–986, doi:10.1175/1520-0477(2001)082<0981:CAATIO>2.3.CO;2.

Park, Y.-H., F. Roquet, and F. Vivier (2004), Quasi-stationary ENSO wave signals versus the Antarctic Circumpolar Wave scenario, *Geophys. Res. Lett.*, *31*, L09315, doi:10.1029/2004GL019806.

Parkinson, C. L., and D. J. Cavalieri (2008), Arctic sea ice variability and trends, 1979–2006, *J. Geophys. Res.*, doi:10.1029/2007JC004558, in press.

Parkinson, C. L., D. J. Cavalieri, P. Gloersen, H. J. Zwally, and J. C. Comiso (1999), Variability of the Arctic sea ice cover 1978–1996, *J. Geophys. Res.*, *104*, 20,837–20,856, doi:10.1029/1999JC900082.

Raphael, M. N. (2007), The influence of atmospheric zonal wave three on Antarctic sea ice variability, *J. Geophys. Res.*, *112*, D12112, doi:10.1029/2006JD007852.

Santer, B. D., T. M. L. Wigley, J. S. Boyle, D. J. Gaffen, J. J. Hnilo, D. Nychka, D. E. Parker, and K. E. Taylor (2000), Statistical significance of trends and trend differences in layer-average atmospheric temperature time series, *J. Geophys. Res.*, *105*(D6), 7337–7356, doi:10.1029/1999JD901105.

Stroeve, J. C., M. C. Serreze, F. Fetterer, T. Arbetter, W. Meier, J. Maslanik, and K. Knowles (2005), Tracking the Arctic's shrinking ice cover: Another extreme September minimum in 2004, *Geophys. Res. Lett.*, *32*, L04501, doi:10.1029/2004GL021810.

Venegas, S. A. (2003), The Antarctic Circumpolar Wave: A combination of two signals?, *J. Clim.*, *16*, 2509–2525, doi:10.1175/1520-0442(2003)016<2509:TACWAC>2.0.CO;2.

Vinnikov, K. Y., D. J. Cavalieri, and C. L. Parkinson (2006), A model assessment of satellite observed trends in polar sea ice extents, *Geophys. Res. Lett.*, *33*, L05704, doi:10.1029/2005GL025282.

White, W. B., and R. G. Peterson (1996), An Antarctic Circumpolar Wave in surface pressure, wind, temperature and sea ice extent, *Nature*, *380*, 699–702, doi:10.1038/380699a0.

Yuan, X., and D. G. Martinson (2000), Antarctic sea ice extent variability and its global connectivity, *J. Clim.*, *3*, 1697–1717, doi:10.1175/1520-0442(2000)013<1697:ASIEVA>2.0.CO;2.

Zhang, J. (2007), Increasing Antarctic sea ice under warming atmospheric and oceanic conditions, *J. Clim.*, *20*, 2515–2529, doi:10.1175/JCLI4136.1.

Zwally, H. J., J. C. Comiso, C. L. Parkinson, D. J. Cavalieri, and P. Gloersen (2002), Variability of Antarctic sea ice 1979–1998, *J. Geophys. Res.*, *107*(C5), 3041, doi:10.1029/2000JC000733.

D. J. Cavalieri and C. L. Parkinson, Cryospheric Sciences Branch/Code 614.1, NASA Goddard Space Flight Center, Greenbelt, MD 20771, USA. (donald.j.cavalieri@nasa.gov)